



# Enhanced Load-Bearing Capacities in Box-Plate Steel Prefabricated Structures: Evaluating the Role of Composite Stiffened Plate Walls and Welding Techniques



Tao Lan<sup>1</sup>, Lili Wu<sup>2</sup>, Ruixiang Gao<sup>1\*</sup>

<sup>1</sup> School of Civil Engineering, Xi'an University of Architecture & Technology, 710055 Xi'an, China

<sup>2</sup> School of Civil Engineering, Qingdao University of Technology, 266520 Qingdao, China

\* Correspondence: Ruixiang Gao (gaoruixiang2020@163.com)

Received: 07-20-2023

Revised: 08-26-2023

Accepted: 09-04-2023

**Citation:** T. Lan, L. L. Wu, and R. X. Gao, "Enhanced load-bearing capacities in box-plate steel prefabricated structures: Evaluating the role of composite stiffened plate walls and welding techniques," *GeoStruct. Innov.*, vol. 1, no. 1, pp. 32–42, 2023. <https://doi.org/10.56578/gsi010103>.



© 2023 by the authors. Licensee Acadlore Publishing Services Limited, Hong Kong. This article can be downloaded for free, and reused and quoted with a citation of the original published version, under the CC BY 4.0 license.

**Abstract:** This study examines innovative box-plate prefabricated steel structures, where stiffened steel plates serve as primary load-bearing walls and floors. In contrast to traditional stiffened steel plate walls, which typically exhibit significant hysteresis, pronounced out-of-plane deformation, and rapid stiffness degradation, these advanced systems demonstrate superior performance. A pivotal feature of these structures is the intensive use of welding to connect stiffened steel plates during assembly. This study introduces a novel composite stiffened steel plate wall, addressing concerns of traditional systems, and executes a comprehensive numerical simulation to assess the influence of welding on joint integrity and overall structural performance. It is observed that the height-to-thickness ratio of steel plate walls significantly influences load-bearing capacity, with a lower ratio yielding enhanced capacity. However, the stiffness ratio of ribs is found to have minimal impact. An increase in bolt quantity and density correlates with improved ultimate bearing capacity. Moreover, the adoption of staggered welding techniques bolsters shear strength, though the positioning of welds has negligible influence on this parameter. The number of welded joints moderately affects shear strength, while the size of staggered welding joints is identified as a crucial factor, with larger sizes leading to more pronounced reductions in shear strength. This study highlights the importance of construction details, particularly in welding practices, in the structural integrity and performance of box-plate prefabricated steel structures. The findings offer significant insights for optimizing design and construction methodologies to maximize the load-bearing capacities of these innovative systems.

**Keywords:** Box-plate prefabricated steel structures; Composite stiffened steel plate walls; Welding numerical simulation; Shear bearing capacity

## 1 Introduction

The architectural philosophy underpinning the design of box-plate steel residential structures, inspired by ship superstructure construction techniques, represents a departure from the standard methodologies applied to traditional steel plate shear walls. In these residential structures, stiffened steel plate walls are employed to bear both horizontal and vertical loads. It has been observed that conventional, non-stiffened steel plate walls underperform, displaying low stiffness and significant deformation. Furthermore, the transportation and subsequent assembly of box-plate modular steel structures necessitate extensive on-site welding, a process linked to structural impairments such as cracks and fractures, as documented in references [1–3]. Thus, the exploration of stiffened steel plate walls with enhanced hysteresis characteristics, increased stiffness, and greater strength, particularly considering the effects of welding on the shear resistance of walls in box-plate modular structures, has become a primary research interest in both engineering and academic domains.

In the design phase of box-plate modular structures, the implementation of various types of stiffened steel plate walls has proven effective in enhancing load-bearing capacity and ductility [4]. Previous studies, involving low-cycle reciprocating load tests, have demonstrated that the integration of stiffening ribs significantly boosts the performance of steel plate walls [5–13]. Analyses conducted by Xu et al. [14] on walls reinforced with vertical stiffening ribs have indicated an elevation in critical shear stress. Previous researches on composite steel plate walls, incorporating

low-cycle reciprocating tests and numerical modeling, suggests that an increase in the height-to-thickness ratio of wall plates intensifies out-of-plane buckling due to expanded tensile zones in the steel plates [15–17]. Additionally, several scholars have underscored the criticality of the welding process in augmenting the ultimate load-bearing capacity of steel plate wall structures. Lee et al. [18], through numerical simulations, have analyzed the mechanical properties of welded joints in high-strength thin-walled steel plate-to-plate connections, identifying significant stress characteristics at the weld toe and elevated tensile residual stress due to welding. Research by Ibrahim et al. [19] on the welding of ultra-thick steel plate walls revealed high residual stress at welds, with peak values approaching the material's yield strength.

Despite the extensive investigation into various stiffened steel plate walls, there remains a discernible research gap concerning composite stiffened steel plate walls that simultaneously bear horizontal and vertical loads. Therefore, this study introduces an innovative composite stiffened steel plate wall, employing low-cycle reciprocating load tests and numerical simulations on wall specimens. Furthermore, this research analyzes the impact of critical parameters during the welding process on the shear resistance of wall panels in box-plate modular steel structures.

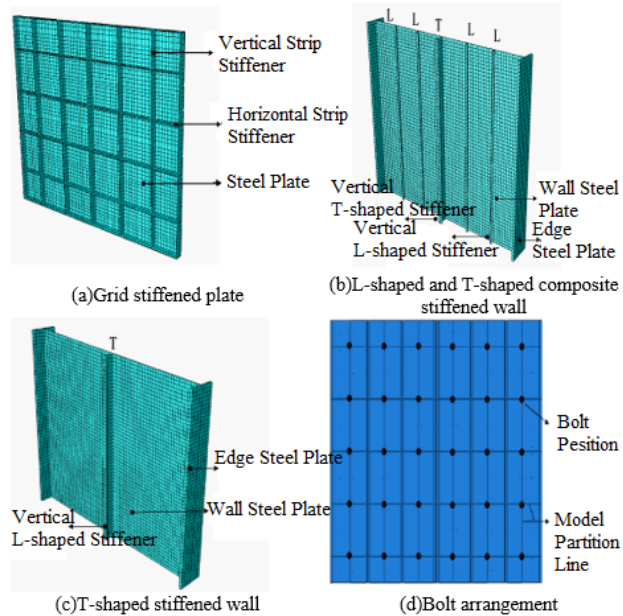


**Figure 1.** Finite element models

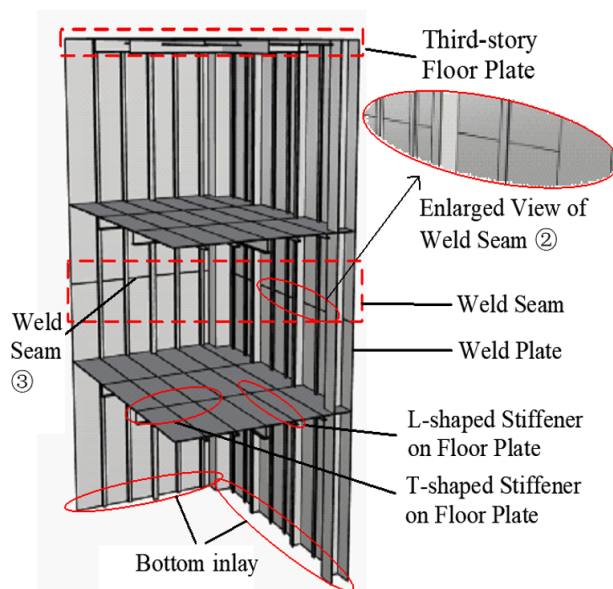


**Figure 2.** Spatial element model considering welding

## 2 Finite Element Model

In this investigation, the specimens are categorized into three types based on the dimensions of the grid stiffening plate bolt holes: SSPW-CP1 (non-slidable specimen), SSPW-CP2 (slidable specimen), and SSPW-CP3 (slidable specimen without L-stiffening rib). The specific dimensions of these specimens are delineated in Table 1. Given the relatively minor impact of the stiffening rib's butt weld on the shear bearing capacity of the wall panel, the welding simulation is focused primarily on the impact of the steel plate's butt weld on the wall panel's load-bearing capacity.

### 2.1 Material Constitutive Relationship

The finite element model employs Q235b steel, with its mechanical properties derived from material property tests. The steel is characterized as isotropic, adopting the von Mises yield criterion for the yielding condition. The hardening rules implemented are isotropic hardening for monotonic loading and kinematic hardening for cyclic loading.

### 2.2 Element Type and Mesh Division

For the modeling, a three-dimensional solid eight-node incompatible hexahedral element (C3D8I) is utilized. The bolted connection between the steel plate wall and the grid stiffening plate is simulated through a point-to-surface coupling method. The division of the mesh in the numerical model is depicted in Figure 1.

In accordance with prior research on box-plate assembly steel structure modules [20], a welded effect spatial cell model is established. This model adopts a 1: 3 scale, comprising three levels, each with dimensions of 1,000 mm in height, 1,800 mm in length, and 1,200 mm in width. The wall and floor plates in the model have a thickness of 3 mm, as demonstrated in Figure 2. A horizontal sectional view of the model, highlighting four weld seams at points A, B, C, and D, is presented in Figure 3. The placement of these weld seams, situated between the first and second levels near the inflection point of the wall plate, is designed to mitigate the adverse effects of welding on the structural integrity.

**Table 1.** Sizes of specimens

Specimen-No.	Component Names	Cross-Sectional Dimensions (mm)	Height (mm) <sup>2</sup>	Quantity	Diameters of Grid-Stiffening Plate-Bolts (mm)
SSPW-CP1	1. Wall steel plate	1320 × 3	1100	1	14
	2. L-shaped-stiffener	L25 × 25 × 3	1100	4	
	3. T-shaped-stiffener	T67 × 17 × 3 × 4	1100	1	
	4. Edge-steel plate	160 × 15	1100	2	
	5. Grid stiffening plate- steel plate	1220 × 3	1000	1	
	6. Grid stiffening plate- vertical-(horizontal)	40 × 3	1000 (1220)	(6) <sup>7</sup>	
SSPW-CP2	1 – 6		Same as SSPW-CP1		30
SSPW-CP3	13456		Same as SSPW-CP2		30

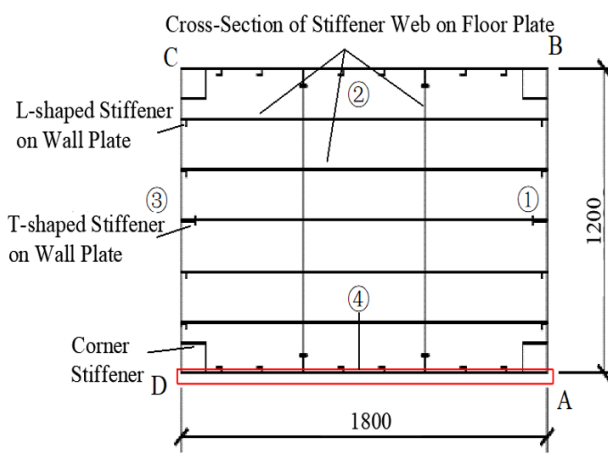


**Figure 3.** Horizontal profile

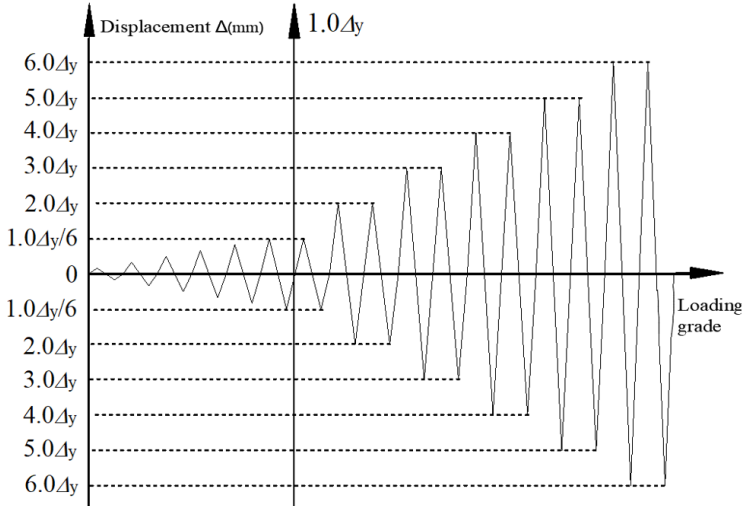


**Figure 4.** Loading system

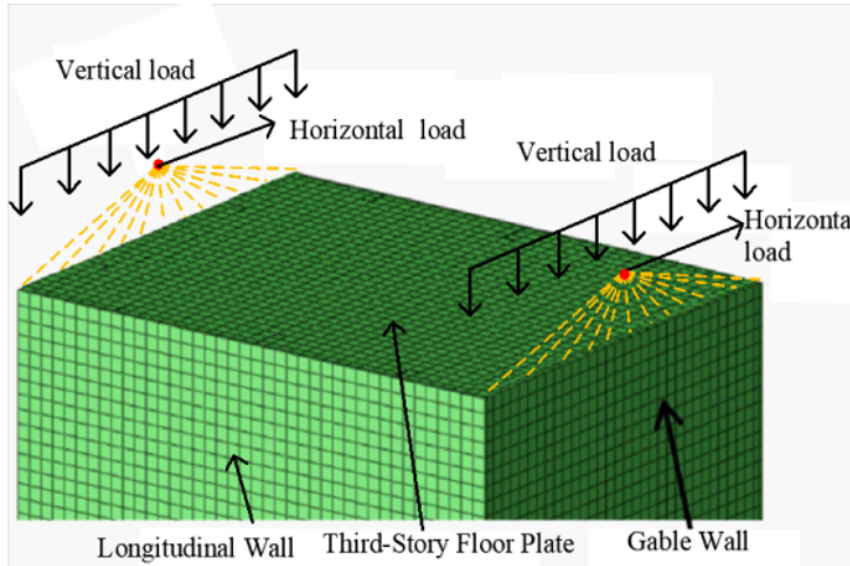


**Figure 5.** Schematic diagram of loading distribution and meshing

### 2.3 Boundary Conditions and Loading Methods

#### 2.3.1 Composite stiffened steel plate wall

In alignment with pertinent experimental protocols, the specimen's base is configured as a fixed end. Uniform horizontal and vertical loads are imposed at the top, accompanied by a translational degree of freedom in the outward direction of the wall's apex. An axial compression ratio of 0.2 is employed, with a consistent vertical load of 220 kN applied to the top of the wall. The horizontal load follows a displacement loading regime, referencing the ATC-24 (1992) seismic code of the United States. Prior to the structure reaching its overall yield point, a load control loading method is utilized. Following the yield, a displacement control loading method is adopted. This loading process is depicted in Figure 4.

#### 2.3.2 Welded butt joints of steel plates considering welding effects

In the numerical simulation, vertical loads are initially transformed into constant uniformly distributed loads. Subsequently, horizontal loads are applied to the structure. The distribution of these loads, taking into account the effects of welding, is visually represented in Figure 5.

### 3 Influence Parameters of Combined Stiffened Steel Plate Wall

#### 3.1 Parameter Selection

Informed by existing literatures [21–25], the primary parameters selected for analysis in this study of composite stiffened steel plate walls include the height-to-thickness ratio of the wall steel plate  $\lambda$ , the stiffness ratio of the rib plate for L-shaped and T-shaped stiffeners  $\eta_L$  and  $\eta_T$ , and the bolt arrangement method. The experimental model SSPW-CP1, noted for its superior seismic performance, is utilized as the benchmark model in this analysis. The selected main parameters are delineated in Table 2.

**Table 2.** Main parameters of the finite element model

Specimen No.	Height-to-thickness ratio of steel plate $\lambda$	Stiffness ratio of rib plate for T-shaped stiffener $\eta_T$	Stiffness ratio of rib plate for L-shaped stiffener $\eta_L$	Bolt arrangement method
SSPW-CP-nB	350	250	20	$6 \times 5$ arrangement
SSPW-CP-1A	300	250	20	$6 \times 5$ arrangement
SSPW-CP-1C	400	250	20	$6 \times 5$ arrangement
SSPW-CP-1D	500	250	20	$6 \times 5$ arrangement
SSPW-CP-1E	600	250	20	$6 \times 5$ arrangement
SSPW-CP-2A	350	200	20	$6 \times 5$ arrangement
SSPW-CP-2C	350	300	20	$6 \times 5$ arrangement
SSPW-CP-2D	350	350	20	$6 \times 5$ arrangement
SSPW-CP-3A	350	250	10	$6 \times 5$ arrangement
SSPW-CP-3C	350	250	40	$6 \times 5$ arrangement
SSPW-CP-3D	350	250	60	$6 \times 5$ arrangement
SSPW-CP-4A	350	250	20	$6 \times 3$ arrangement
SSPW-CP-4C	350	250	20	Plum blossom arrangement

Note: n=1,2,3,4.

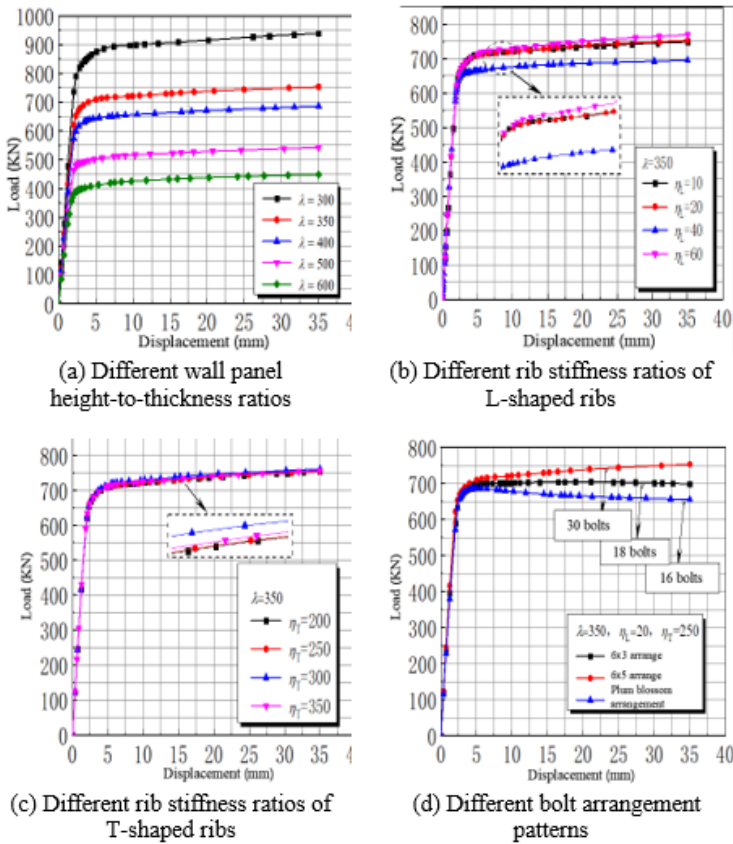


**Figure 6.** Load - displacement curves of each parameter

### 3.2 Parameter Analysis

#### 3.2.1 Impact on load bearing capacity

Load-displacement curves, obtained under unidirectional loading for models with varying height-to-thickness ratios, are presented in subgraph (a) of Figure 6. Each curve delineates an elastic phase, followed by a yield phase, and concluding with an elastoplastic phase. For height-to-thickness ratios  $\lambda$  ranging from 300 to 600, the corresponding ultimate loads are identified as 938.60 kN, 753.20 kN, 685.90 kN, 542.20 kN, and 448.40 kN, respectively. An inverse relationship is noted between the height-to-thickness ratio and the yield load of the composite stiffened steel plate wall. A height-to-thickness ratio  $\lambda$  between 300 and 400 is recommended for optimal structural load capacity, safety, and cost-efficiency.

The influence of varying stiffness ratios of the rib plates is illustrated in subgraphs (b) and (c) of Figure 6. For stiffness ratios  $\eta_z$  at 10, 20, 40, and 60, the ultimate loads are 748.75 kN, 753.31 kN, 695.47 kN, and 769.24 kN, respectively. This data suggests that the stiffeners moderately enhance the load-bearing capacity of the walls. The stiffness ratio of the L-shaped stiffener  $\eta_z$  is thus recommended to be within the range of 20-30, with a stiffness ratio of the T-shaped stiffener  $\eta_z$  suggested between 250 and 300.

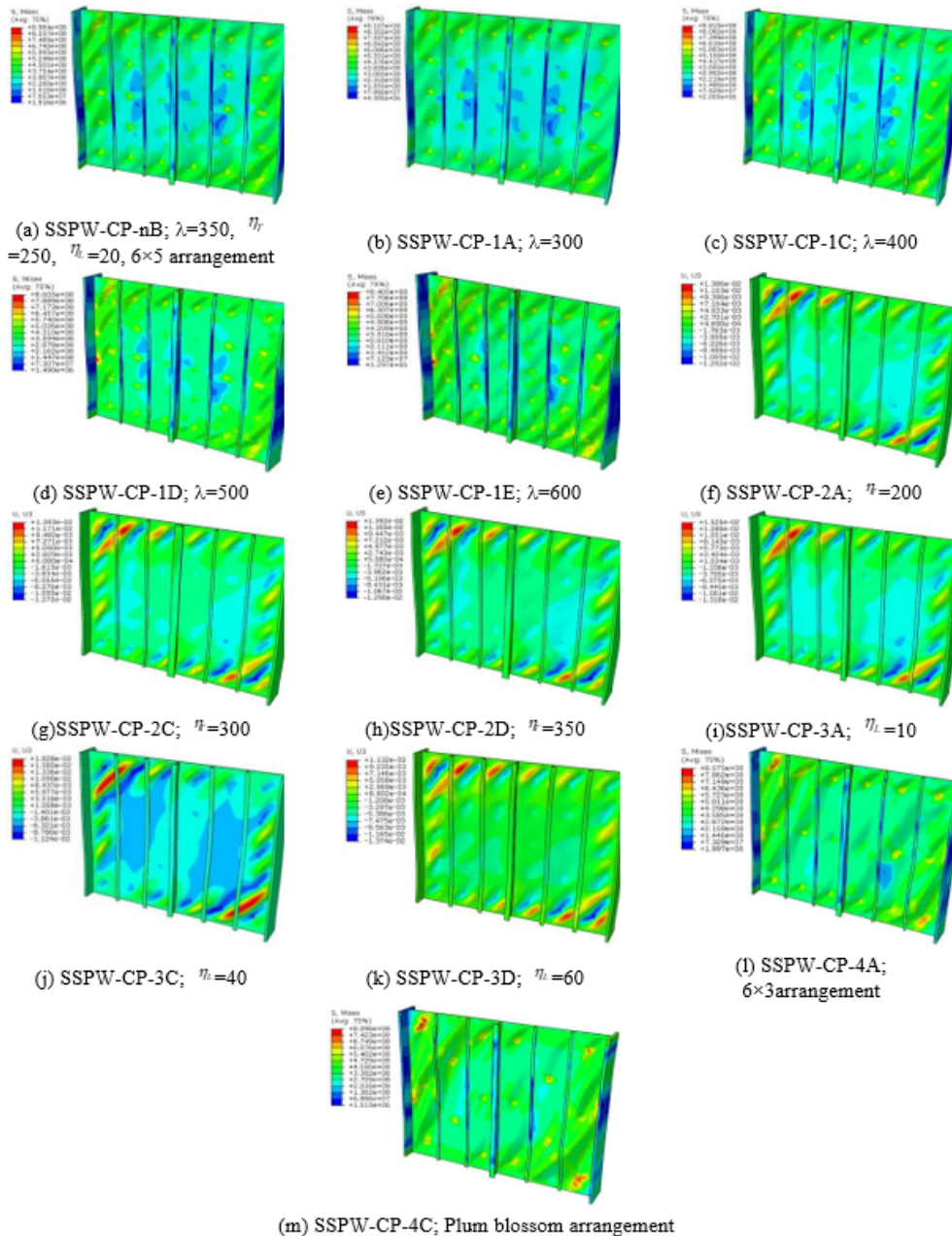


**Figure 7.** Mises stress clouds of different wall specimens

Subgraphs (d) of Figure 6 displays the load-displacement curves for different bolt arrangement patterns. The ultimate loads for the plum blossom arrangement (16 bolts), 6×3 arrangement (18 bolts), and 6×5 arrangement (30 bolts) are 655.21 kN, 698.45 kN, and 753.24 kN, respectively. The results indicate that an increased number of bolts correlates with higher ultimate loads. The load-displacement curve for the 30-bolt arrangement exhibits a consistent upward trend, in contrast to the downward trends observed for the 16 and 18-bolt arrangements.

### 3.2.2 Impact on failure modes

Mises stress contour maps, showcasing the response of the composite stiffened steel plate wall to a displacement of 35 mm under unidirectional loading, are illustrated in Figure 7. Subgraphs (a), (b), (c), (d), and (e) of Figure 7 reveal that higher height-to-thickness ratios  $\lambda$  result in reduced yield loads of the wall. At a ratio of 300, the tension band is primarily concentrated at the top and bottom of the panel, with peak stress values at the panel edges. Beyond a ratio of 500, changes in tension band distribution become evident, marked by localized tensile stresses at the upper left and lower right corners of the wall.

Subgraphs (a), (i), (j), and (k) of Figure 7 display stress distributions with minor variations in stress values across different zones in the model. It is observed that the highest stresses are located at the edges, while the middle sections exhibit lower stress levels. Higher stiffness ratios do not significantly enhance structural mechanical performance, as shown in subgraphs (a), (f), and (g) of Figure 7. The tension bands in different T-shaped rib configurations predominantly distribute across various panels, with edge stresses in the walls being higher than those in the middle. The maximum stress values across the models are relatively comparable.

Different bolt arrangements notably influence local stress distribution, as depicted in subgraphs (a), (l), and (m) of Figure 7. The 6×3 bolt arrangement model shows tension primarily around the panel, with peak stress at the bolt connection points. In the 6×5 bolt arrangement model, the tension band is more dispersed within various panels, highlighting the reinforcing effect of the steel plate wall due to the greater number of bolts.

In conclusion, a higher height-to-thickness ratio  $\lambda$  correlates with reduced shear bearing capacity, while an increased number of bolts significantly enhances load-bearing capacity. Thus, selecting an appropriate height-to-thickness ratio and arranging bolts effectively can positively influence the shear bearing capacity of the wall.

## 4 Influence Parameters of Welding Effect

### 4.1 Parameter Selection

In the context of welding box-plate steel structures, the effects of welding are influenced by several factors, including steel type and material thickness. This study also considers the welding sequence, the quantity and positioning of welds, and the size of staggered welding joints as crucial parameters impacting welding effectiveness. Table 3 delineates these specific parameters.

**Table 3.** Finite element model parameters

Model No.	Welding Sequence	Number and Location of Welds	Welding Staggered Joint Size (mm)
1	Continuous Sequential Welding		
2	Continuous Reverse Sequential Welding	①, ②, ③, ④	
3	Segmented Step-back Welding		
4		①, ②, ④	0
5		①, ②, ③	
6		②, ④	
7	Segmented Step-back Welding	①, ③	
8			0.5
9		①, ③	1.0
10			1.5
11			2.0

### 4.2 Parameter Analysis

The computational results for the selected welding parameters are compiled in Table 4 and Table 5. These tables indicate the yield bearing capacity  $P_y$  and the ultimate bearing capacity  $P_u$  of the spatial units. Load-displacement curves corresponding to these parameters are depicted in Figure 8, Figure 9, and Figure 10.

#### 4.2.1 Welding sequence

Figure 8 illustrates that, in comparison to continuous sequential welding and continuous reverse sequential welding, segmented step-back welding exhibits a superior shear carrying capacity, enhanced stability in deformation, and improved ductility. Consequently, the segmented step-back welding method is recommended for the assembly of box-plate modular steel structures.

**Table 4.** Calculation results of different weld numbers and positions

Model No.	Weld Number and Position	$P_y$ (kN)	$P_u$ (kN)	$P_y/P_u$
3	①, ②, ③, ④	991.5	1120.6	88.5%
4	①, ②, ④	1044.2	1161.9	89.9%
5	①, ②, ③	1089.7	1179.4	92.4%
6	②, ④	1158.9	1288.7	89.9%
7	①, ③	1177.7	1312.8	89.7%

**Table 5.** Results of different welding staggered joint sizes

Model No.	Welding Staggered Joint Size (mm)	$P_y$ (kN)	$P_u$ (kN)	$P_y/P_u$
7	0	1177.7	1312.8	89.7%
8	0.5	1148.7	1267.9	90.6%
9	1.0	1099.4	1196.3	91.9%
10	1.5	976.0	1054.9	92.5%
11	2.0	826.8	884.2	93.5%

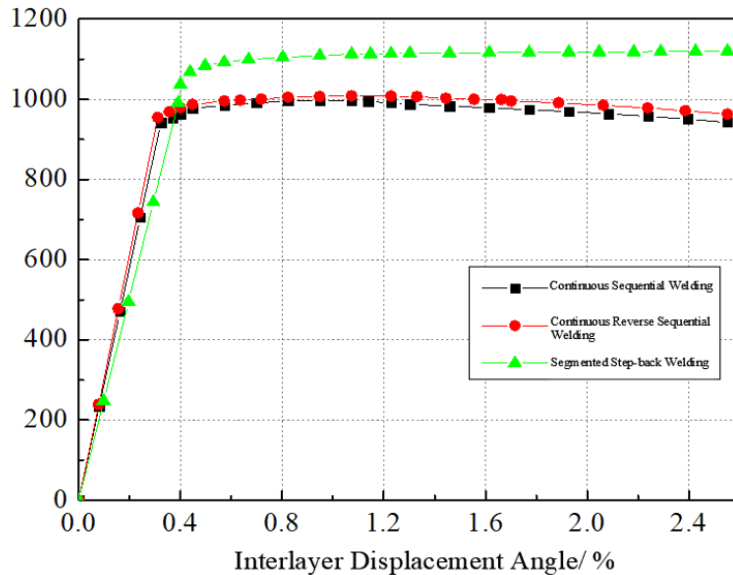


**Figure 8.** Load displacement curves of space elements with different welding sequences

#### 4.2.2 Number and location of welds

Analysis of Figure 9 demonstrates that the load-displacement curves for the five comparative test groups exhibit basic consistency. In terms of bearing capacity and stiffness, Models 4 and 5 yield similar results. Specifically, relative to Model 3, the stiffness in Models 4 to 7 increased by 17.3%, 17.7%, 12.8%, and 9.3% respectively. Correspondingly, their ultimate bearing capacities enhanced by 3.9%, 5.2%, 15.0%, and 17.1%. Thus, it is evident that the number of welds significantly influences the ultimate bearing capacity of the spatial unit, while the position of the welds has a minimal impact.

#### 4.2.3 Welding staggered joint size

Figure 10 indicates that load-displacement curves for varying welding staggered joint sizes (Models 7 to 11) exhibit a similar trend. In the elastic stage, due to the smaller stiffness of Model 11, a lower shear bearing capacity and larger deformation are observed, resulting in a gentler curve slope. During this stage, the curves of the other models nearly coincide. Post-elastic stage, the yield displacement of the models marginally increases with the enlargement of welding staggered joint size, while both yield load and ultimate load discernibly decrease. As shown in Table 5, larger welding staggered joint sizes correspond to higher strength-to-ductility ratios and reduced ductility of the structure. Compared to Model 7, the ultimate bearing capacities of Models 8 to 11 decreased by 3.3%, 8.7%, 19.5%, and 32.4%, respectively. Furthermore, an increase in welding staggered joint size within the spatial unit steel wall markedly diminishes the ultimate bearing capacity of the spatial unit, accentuating the critical role of welding staggered joint size in influencing the bearing capacity.

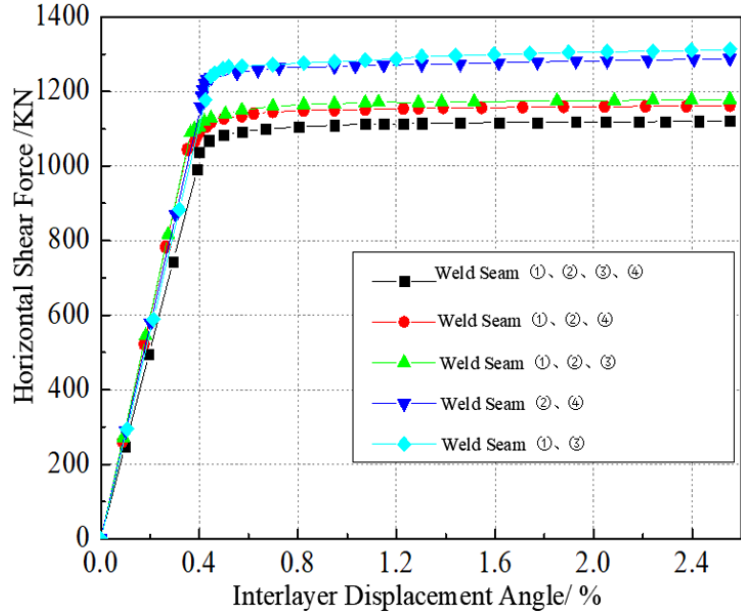


**Figure 9.** Load-displacement curves of space elements with different weld numbers and positions

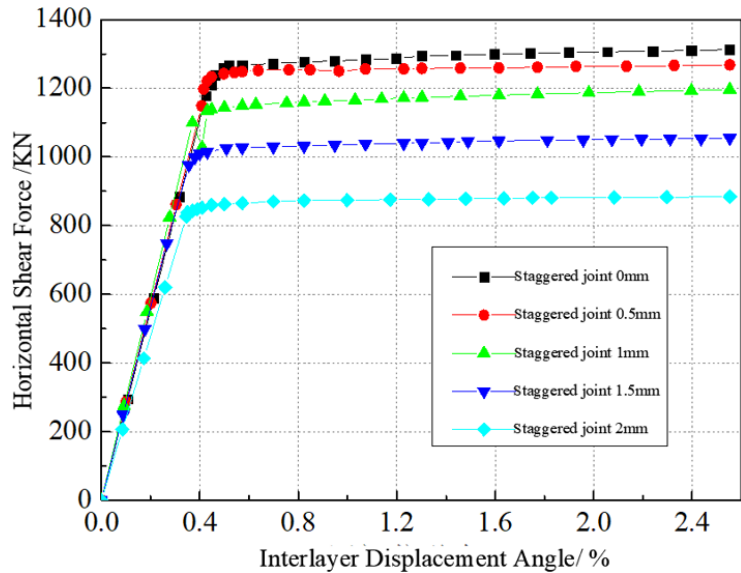


**Figure 10.** Load-displacement curves of space elements with different welding staggered joint sizes

## 5 Conclusions

The investigation has determined optimal parameter values for composite stiffened steel plate walls. It is recommended that the height-to-thickness ratio of the steel plate should be maintained between 300 and 400. For L-shaped ribs, a stiffness ratio between 20 and 30 is advisable, while for T-shaped ribs, a stiffness ratio ranging from 250 to 300 is suggested. A full bolt arrangement is also recommended. Of these parameters, the height-to-thickness ratio of the steel plate exerts the most substantial impact on the shear bearing capacity of the stiffened steel plate wall, while the stiffness ratio of the ribs has the least influence on the ultimate load capacity.

The segmented step-back welding method emerges as the optimal welding sequence. The number of welds significantly affects the horizontal load capacity of the spatial unit structure, underscoring the need to minimize weld numbers in the design phase. The welding staggered joint size is identified as a pivotal influencing factor. During assembly, measures such as the use of welding fixtures should be implemented to reduce the pre-welding misalignment of the steel plates. Furthermore, it is advisable to set the limit value of the welding staggered joint size during the welding assembly process of the steel plate wall at 1.3 mm.

## Data Availability

The data used to support the findings of this study are available from the corresponding author upon request.

## Conflicts of Interest

The authors declare that there are no conflicts of interest regarding the publication of this article.

## References

- [1] T. Skriko, A. Ahola, and T. Björk, “Overview on the digitized production of welded steel structures,” *Weld. World*, vol. 66, no. 4, pp. 1–15, 2022. <https://doi.org/10.1007/s40194-021-01224-x>
- [2] X. Qu, C. Qin, G. Sun, and Y. Xie, “Research on fracture of steel structure welded joint based on micro-mechanism,” *Structures*, vol. 43, pp. 434–448, 2022. <https://doi.org/10.1016/j.istruc.2022.06.048>
- [3] S. Jin, H. Ohmori, and S. Lee, “Optimal design of steel structures considering welding cost and constructability of beam-column connections,” *J. Constr. Steel Res.*, vol. 135, pp. 292–301, 2017. <https://doi.org/10.1016/j.jcsr.2017.03.020>
- [4] Z. Yin, Z. Huang, and H. Zhang, “Experimental study on steel plate shear walls with partially encased composite columns composed of thin steel plate,” *Ksce J. Civ. Eng.*, vol. 27, no. 3, pp. 1118–1135, 2023. <https://doi.org/10.1007/s12205-023-0017-0>
- [5] A. Khaloo, M. Foroutani, and A. Ghamari, “Influence of crack on the steel plate shear walls strengthened by diagonal stiffeners,” *Struct. Des. Tall Spec.*, vol. 29, no. 6, p. e1716, 2020. <https://doi.org/10.1002/tal.1716>
- [6] N. Paslar, A. Farzampour, and N. Chalangaran, “Parametric study on the partially interconnected steel plate shear walls with stiffeners,” *Structures*, vol. 53, pp. 749–763, 2023. <https://doi.org/10.1016/j.istruc.2023.04.100>
- [7] G. Fan, J. Men, Y. Fu, T. Lan, and J. Wang, “Seismic behavior of steel plate wall with stiffeners and concrete slab in the box-plate steel structure,” *J. Build. Eng.*, vol. 69, p. 106239, 2023. <https://doi.org/10.1016/j.jobe.2023.106239>
- [8] A. Khaloo, A. Ghamari, and M. Foroutani, “On the design of stiffened steel plate shear wall with diagonal stiffeners considering the crack effect,” *Structures*, vol. 31, pp. 828–841, 2021. <https://doi.org/10.1016/j.istruc.2021.02.027>
- [9] J. G. Yu, X. T. Feng, B. Li, and Y. T. Chen, “Effects of non-welded multi-rib stiffeners on the performance of steel plate shear walls,” *J. Constr. Steel Res.*, vol. 144, pp. 1–12, 2018. <https://doi.org/10.1016/j.jcsr.2018.01.009>
- [10] J. G. Yu, L. M. Liu, B. Li, J. P. Hao, X. Gao, and X. T. Feng, “Comparative study of steel plate shear walls with different types of unbonded stiffeners,” *J. Constr. Steel Res.*, vol. 159, pp. 384–396, 2019. <https://doi.org/10.1016/j.jcsr.2019.05.007>
- [11] H. C. Guo, Y. L. Li, and G. Liang, “Experimental study of cross stiffened steel plate shear wall with semi-rigid connected frame,” *J. Constr. Steel Res.*, vol. 135, pp. 69–82, 2017. <https://doi.org/10.1016/j.jcsr.2017.04.009>
- [12] F. Es'haghioskui, M. Hoseinzadeh Asl, Y. Hosseinzadeh, and E. Gallego, “Experimental and numerical investigation of a new type of steel plate shear wall with diagonal tension field guiding stiffeners,” *J. Build. Eng.*, vol. 76, p. 107181, 2023. <https://doi.org/10.1016/j.jobe.2023.107181>
- [13] O. Haddad, N. H. Ramli Sulong, and Z. Ibrahim, “Cyclic performance of stiffened steel plate shear walls with various configurations of stiffeners,” *J. Vibroeng.*, vol. 20, no. 1, pp. 459–476, 2018. <https://doi.org/10.21595/jve.2017.18472>
- [14] Z. Y. Xu, G. S. Tong, and L. Zhang, “Stiffness demand on stiffeners of vertically stiffened steel plate shear wall,” *J. Struct. Eng.*, vol. 146, no. 6, p. 06020005, 2020. [https://doi.org/10.1061/\(ASCE\)ST.1943-541X.0002636](https://doi.org/10.1061/(ASCE)ST.1943-541X.0002636)
- [15] N. Wang, F. Zhou, H. T. Xu, and Z. Y. Xu, “Experimental study on steel-plate composite wall-to-foundation connections subjected to combined axial compression and cyclic lateral-force,” *Eng. Struct.*, vol. 207, p. 110205, 2020. <https://doi.org/10.1016/j.engstruct.2020.110205>
- [16] T. Ou, D. Y. Wang, Y. S. Zhang, and H. Li, “Parametric study on cyclic behavior of modular assembly composite walls with connection to boundary beam,” *Int. J. Steel Struct.*, vol. 21, no. 5, pp. 1605–1619, 2021. <https://doi.org/10.1007/s13296-021-00523-9>
- [17] Z. G. Cao, Z. C. Wang, P. Du, H. Liu, and F. Fan, “Research on steel plate shear walls stiffened with x-shaped restrainers: Hysteretic behavior and effect of height-to-thickness ratio of steel plate,” *Thin. Wall. Struct.*, vol. 144, p. 106316, 2019. <https://doi.org/10.1016/j.tws.2019.106316>
- [18] C. K. Lee, S. P. Chiew, and J. Jiang, “Residual stress study of welded high strength steel thin-walled plate-to-plate joints part 2: Numerical modeling,” *Thin. Wall. Struct.*, vol. 59, pp. 120–131, 2012. <https://doi.org/10.1016/j.tws.2012.04.001>
- [19] O. A. Ibrahim, D. G. Lignos, and C. A. Rogers, “Proposed modeling approach of welding procedures for heavy steel plates,” *Eng. Struct.*, vol. 127, pp. 18–30, 2016. <https://doi.org/10.1016/j.engstruct.2016.08.022>

- [20] M. M. Alinia and R. S. Shirazi, “On the design of stiffeners in steel plate shear walls,” *J. Constr. Steel Res.*, vol. 65, no. 10-11, pp. 2069–2077, 2009. <https://doi.org/10.1016/j.jcsr.2009.06.009>
- [21] Y. Q. Suo, S. G. Fan, C. X. Li, S. R. Zeng, and C. L. Liu, “Parametric analysis on hysteresis performance and restoring force model of lyp steel plate shear wall with two-side connections,” *Int. J. Steel Struct.*, vol. 20, no. 6, pp. 1960–1978, 2020. <https://doi.org/10.1007/s13296-020-00400-x>
- [22] J. Hou, L. H. Guo, H. Zhong, S. Gao, and J. Chen, “Hysteretic behavior of partially buckling-restrained steel plate shear walls with coupled restraining steel tubes,” *Eng. Struct.*, vol. 276, p. 115388, 2023. <https://doi.org/10.1016/j.engstruct.2022.115388>
- [23] J. Z. Tong, L. Q. Wang, J. Hou, Q. H. Li, S. L. Xu, and G. S. Tong, “Flexural design of restraining panels in buckling-restrained steel plate shear walls considering high-order buckling modes,” *Thin. Wall. Struct.*, vol. 184, p. 110488, 2023. <https://doi.org/10.1016/j.tws.2022.110488>
- [24] S. G. Fan, R. M. Ding, S. R. Zeng, C. X. Li, and C. L. Liu, “Parametric analysis on elastic buckling performance of low yield point steel plate shear wall with two-side connections,” *Int. J. Steel Struct.*, vol. 20, no. 6, pp. 1945–1959, 2020. <https://doi.org/10.1007/s13296-020-00391-9>
- [25] L. H. Guo, M. M. Jia, R. Li, and S. M. Zhang, “Hysteretic analysis of thin steel plate shear walls,” *Int. J. Steel Struct.*, vol. 13, no. 1, pp. 163–174, 2013. <https://doi.org/10.1007/s13296-013-1015-8>